1988ApJ...326..110B

THE ASTROPHYSICAL JOURNAL, 326:110–124, 1988 March 1
© 1988. The American Astronomical Society. All rights reserved. Printed in U.S.A.

THE COLLECTIVE EMISSION OF ELECTROMAGNETIC WAVES FROM ASTROPHYSICAL JETS: LUMINOSITY GAPS, BL LACERTAE OBJECTS, AND EFFICIENT ENERGY TRANSPORT

D. N. BAKER AND JOSEPH E. BOROVSKY
University of California, Los Alamos National Laboratory
GREGORY BENFORD
University of California, Irvine
AND
JEAN A. EILEK
New Mexico Institute of Mining and Technology
Received 1987 February 6; accepted 1987 August 12

ABSTRACT

A model of the inner portions of astrophysical jets is constructed in which a relativistic electron beam is injected from the central engine into the jet plasma. This beam drives electrostatic plasma wave turbulence, which leads to the collective emission of electromagnetic waves. The emitted waves are beamed in the direction of the jet axis, so that end-on viewing of the jet yields an extremely bright source (BL Lacertae object). The relativistic electron beam may also drive long-wavelength electromagnetic plasma instabilities (firehose and Kelvin-Helmholtz) that jumble the jet magnetic field lines. After a sufficient distance from the core source, these instabilities will cause the beamed emission to point in random directions and the jet emission can then be observed from any direction relative to the jet axis. This combination of effects may lead to the gap turn-on of astrophysical jets. The collective emission model leads to different estimates for energy transport and the interpretation of radio spectra than the conventional incoherent synchrotron theory.

Subject headings: BL Lacertae objects — galaxies: jets — plasmas — radiation mechanisms — radio sources: variable

I. INTRODUCTION

Incoherent synchrotron radio wave emission is a widely accepted explanation for the observed electromagnetic signals from astrophysical jets. The synchrotron model is well developed (Gould 1979), and, by adding some assumptions, this model allows an inversion of the observed radio spectrum to give the densities, energy spectra, and radiative lifetimes of relativistic electrons (De Young 1984). Furthermore, the assumption of particle field energy equipartition, when added to the synchrotron model, allows jet magnetic field strengths and jet total energy content values to be obtained. Such information can be used to determine the power requirements for the jet central engines within stellar systems, active galactic nuclei, and quasars.

In considering some of the morphological aspects of jets—both stellar (e.g., SS 433) and extragalactic—we have been led to consider the role of coherent emission mechanisms in the astrophysical context. A jet model based upon coherent emission provides a relatively natural and plausible explanation of the luminosity gaps that are quite characteristic of both galactic and extragalactic jets (Bridle and Perley 1984; R. M. Hjellming 1985, private communication). A coherent emission model also predicts a higher rate of energy extraction per particle for jet electron populations than is generally considered for incoherent synchrotron emission models. The coherent emission model also explains the major properties of BL Lacertae objects and has possible pertinence to the superluminal motion of radio-bright objects in compact jet sources.

Our suggestion of a role for coherent processes in jets stems from our experience with plasma processes in planetary magnetospheres and in laboratory plasma devises. Seldom, in these situations, are single-particle emission processes energetically important; usually collective emission mechanisms completely overwhelm the incoherent processes.

In § II we will give a brief introduction to several collective plasma effects, and we will review coherent emission mechanisms that have been studied in situ in space plasmas. We then describe laboratory plasma experiments that efficiently produce high-power radiation of short wavelengths. With these ideas as background, we apply the coherent emission model to astrophysical jets in § III, with the emphasis on explaining the structure and morphology of the inner portions of jets. As elaborated upon in § IV, our major conclusions are that (1) BL Lacertae objects are the result of forward-beamed Langmuir wave–induced emission; (2) that luminosity gap turn-ons in jets result from long-wavelength instabilities that turn the forward-beamed emission into the observer's line of sight; and (3) that the stronger radiation rate per electron, along with the possibility of most of the electron population not radiating, modifies estimates of electron lifetimes and energetics in the jets and extended sources.

II. COLLECTIVE EMISSION FROM SPACE AND LABORATORY PLASMAS

To introduce the reader to plasma emission processes and to serve as a lead-in to a model of astrophysical jet emission, some well-studied examples of collective electromagnetic radiation emission from space and laboratory plasmas are discussed.

In § II*a*, we will overview magnetospheric plasmas, where radio wave emission is clearly dominated by collective processes. Because these plasmas are inherently nonrelativistic, the

© American Astronomical Society • Provided by the NASA Astrophysics Data System

1988ApJ...326..110B

collective emission from them is confined to narrow-frequency bands near the electron cyclotron frequency. Consequently, these particular mechanisms are not directly applicable to astrophysical jet observations, since these jets are characterized by radio emission that is thought to be at frequencies well above the cyclotron frequencies. In § II*b*, we will discuss collective emission from laboratory plasmas. The experiments described are selected for their applicability to the jet model that we will present in § III.

a) Coherent Emission Processes in Space Plasmas

Collective electromagnetic emission mechanisms are considered to be either direct or indirect. In a direct mechanism, the free-energy source in the plasma couples directly to the electromagnetic wave that is emitted. In an indirect mechanism, the free energy source couples to the emitted electromagnetic wave only through other plasma waves. Thus, the indirect process is nonlinear and, owing to the multistage processes necessary, it usually is less efficient at producing electromagnetic wave emission from internal (free) energy than a direct process would be. This low electromagnetic wave production efficiency is due to the fact that much of the system internal energy is converted to plasma waves and plasma heating; such dissipation is not generally very effective in producing electromagnetic emissions. Most collective electromagnetic wave emission is associated with electron bunches performing Larmor motion; hence the wave frequencies are associated with the electron cyclotron frequency $\omega_{ce} = eB/m_e c$. In a plasma, most electromagnetic waves propagate as free-space modes when their frequencies exceed the electron plasma frequency $\omega_{pe} = (4\pi ne^2/m_e)^{1/2}$. Thus, electromagnetic radiation from a magnetized plasma is conveniently considered in the two extreme limits of the ω_{ce}/ω_{pe} ratio. In the high-density and/or low magnetic field limit, such that $\omega_{pe}/\omega_{ce} \gg 1$, radiation generated directly at frequencies near ω_{ce} cannot easily escape the plasma, and, hence, any escaping radiation must be produced by indirect processes: in general, mode-mode plasma wave coupling occurs to produce such electromagnetic waves (Nicholson 1983). In the opposite limit, where $\omega_{pe}/\omega_{ce} \ll 1$, electromagnetic radiation that is capable of escaping the plasma can be produced both by indirect and direct processes.

Direct emission mechanisms in plasmas include a wide range of stimulated emission processes (Bekefi 1966). Microwave amplification by stimulated emission of radiation (a maser) ordinarily is thought of in terms of a resonant medium in which there is maintained a large population of atoms in an excited level. The subsequent passage through the active medium of a primary wave of frequency near the excited state transition frequency stimulates emission, and the emitted photons will carry definite phase relations. With such a population inversion in the medium, exponential amplification of the wave is possible and coherent emission is achievable.

In the electron cyclotron maser (Sprangle and Drobot 1977), the emission is driven by electrons with a "loss cone anisotropy" (Melrose, Hewitt, and Dulk 1984). Such an anisotropy can develop when the electrons are confined on magnetic flux tubes having a magnetic mirror geometry; in a planetary magnetosphere, the loss cone feature results when particles with small pitch angles are precipitated into the atmosphere and thus are lost from the plasma distribution function. This velocity space "hole" in the electron distribution is a strong source of free energy that may drive electromagnetic plasma wave instabilities. The theory of the electron cyctron maser

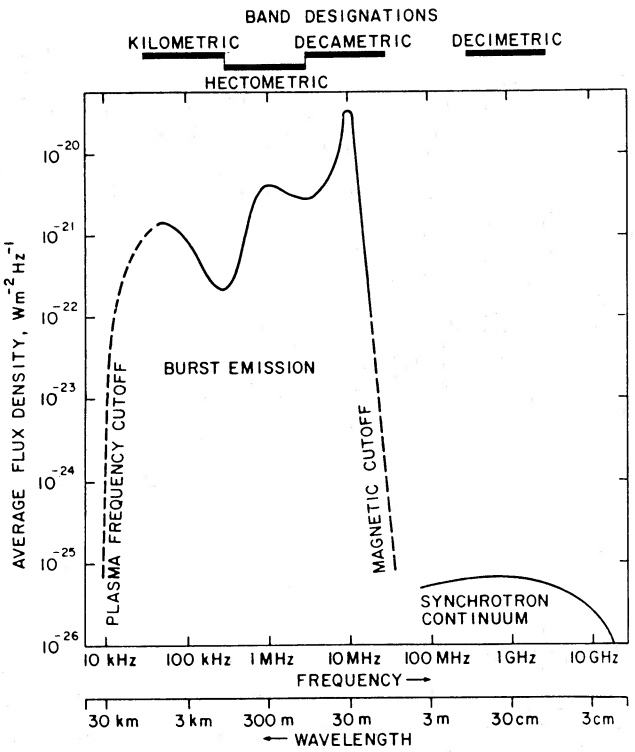

FIG. 1—Average power flux density spectrum of Jupiter's nonthermal magnetospheric radio emissions. Burst-component flux densities were averaged over inactive as well as active periods; the instantaneous spectrum may appear considerably different. The highest burst peaks attained values one to two orders of magnitude above the curve. Solid line part of the burst-component curve is from Schauble and Carr (unpublished). Synchrotron-component curve is the difference between the total and thermal emission spectra. Flux densities are normalized to a distance of 4.04 A.U. (from Carr, Desch, and Alexander 1983).

(Wu and Lee 1979; Melrose, Hewitt, and Dulk 1984) suggests that for small ω_{pe}/ω_{ce} the fastest growing emission mode is the fundamental extraordinary (x) mode electromagnetic wave in a narrow frequency range just above ω_{ce}. Further, the theory suggests that the stimulated emission is in a narrow range of wave normal angles that is nearly perpendicular to the local magnetic field line.

The most powerful radio emission produced in the Earth's magnetosphere, viz., auroral kilometric radiation (AKR), is now believed to be due to the electron cyclotron maser mechanism (Melrose, Hewitt, and Dulk 1984). Essentially the same mechanism is thought to produce the decametric radio emission (DAM) at Jupiter and also the Saturnian kilometric radiation (SKR) (Hewitt, Melrose, and Ronnmark 1981). In all of these cases, a partially coherent, beamed collective emission mechanism is clearly indicated.

Figure 1 is a summary of the radio emission from Jupiter (Carr, Desch, and Alexander 1983), where the average detected radio flux is shown as a function of frequency (and wavelength). The top of the figure also indicates the band designation conventions for the Jovian emission. The hundreds of kHz to tens of MHz emission is produced by the maser effect discussed above; the power levels, spectra, polarization, and beaming properties of this emission all demand such a source. In contrast, the hundreds of MHz to tens of GHz emission is produced by incoherent synchrotron radiation from highly relativistic electrons trapped in the equatorial regions of the

© American Astronomical Society • Provided by the NASA Astrophysics Data System

1988ApJ...326..110B

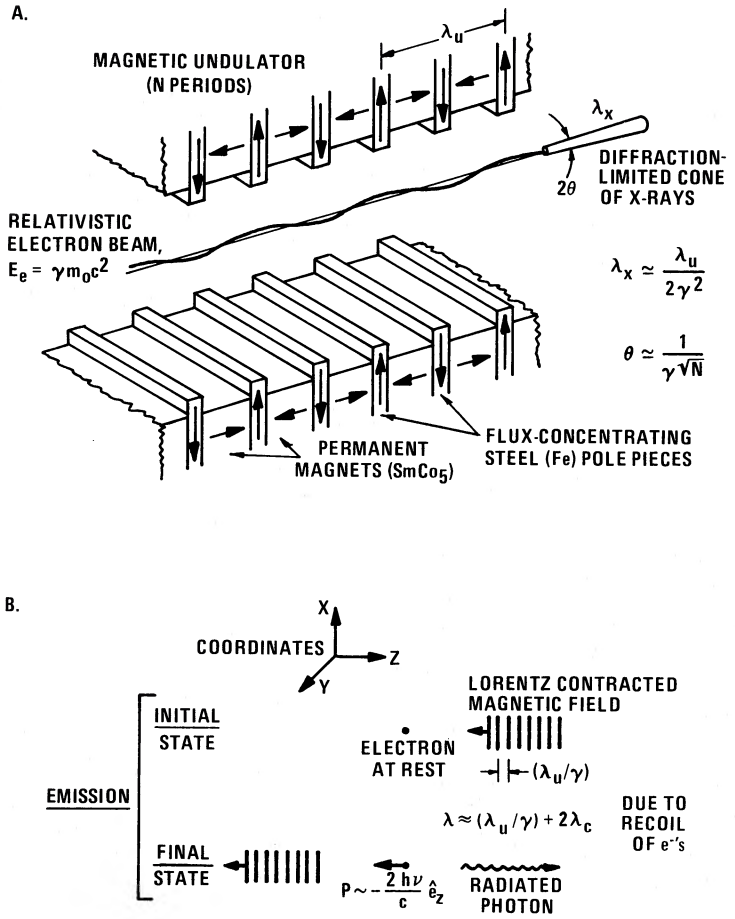

FIG. 2.—(*a*) Partially coherent electromagnetic waves are produced when a narrow beam of relativistic electrons passes through a periodic transverse magnetic field "wiggler." This free electron laser radiation is relativistically contracted to short wavelengths and focused within a narrow forward cone (adapted from Attwood, Halbach, and Kim 1985). (*b*) Illustration of the Compton scattering analogy for emitted radiation during the interaction of a relativistic electron and a wiggler field as in (*a*). (After Elias *et al.* 1976.)

inner magnetosphere. As is clear from the figure, the coherent mechanism is capable of producing radiation levels many orders of magnitude larger than the incoherent synchrotron emission. Quite similar considerations apply in the terrestrial and Saturnian magnetospheres and also probably apply to solar microwave bursts (Melrose, Hewitt, and Dulk 1984).

b) Collective Emission from Laboratory Plasmas

In addition to the important role of stimulated emissions in the space physics domain, such emissions are also important in laboratory plasmas. Laboratory plasma experiments are attractive in that they can be well diagnosed and in that the plasma parameters can be systematically varied. Of pertinence to astrophysical jets, some of these experiments concern the emission of electromagnetic waves from plasmas containing relativistic electrons.

i) *The Free Electron Laser*

The principles behind the free electron laser (FEL) lie in the interaction between a relativistic electron beam and a magnetic "wiggler" system, as depicted in Figure 2*a* (Granatstein and Sprangle 1977; Attwood, Halbach, and Kim 1985). Here a beam of high-energy electrons with energy $\gamma m_0 c^2$ passes between permanent magnets of alternating polarity and periodicity λ_u. As the electrons experience the periodic vertical magnetic field they undergo an oscillatory motion in the horizontal plane. These oscillating charges moving relativistically will generate synchrotron radiation that is sharply peaked in the forward direction. The spatial period of the electron oscillation will be equal to λ_u, but, when observed from within the relativistic emission cone, the radiation wavelength is strongly contracted from the wiggler wavelength. Furthermore, the electrons in the relativistic beam bunch up because of a resonance interaction with the Doppler-shifted wiggler. The emitted radiation is therefore very intense because of interference effects. This arrangement may be thought of as another form of stimulated emission (as in the maser case), where, in the free electron laser, wave energy is extracted from the free energy of the relativistic electron beam.

Amplification due to stimulated emission of radiation in a periodic transverse magnetic field is similar to the process of stimulated inverse Compton scattering (Kapitza and Dirac 1933; Pantell, Soncini, and Puthoff 1968). If any radiation is present during the interaction of the electrons with the wiggler field, there is a probability for stimulated radiation and absorption. The transition rates for stimulated emission and absorption are similar, but the two processes occur at slightly different frequencies. Because of this frequency difference, there is a net amplification due to stimulated emission (Madey 1971).

To expand upon the Compton-scattering analogy, let us

© American Astronomical Society • Provided by the NASA Astrophysics Data System

1988ApJ...326..110B

consider the motion of a relativistic electron through a periodic magnetic field structure (Fig. 2*b*). In the electron rest frame, the electron sees the periodic magnetic field as a traveling wave of (contracted) wavelength λ_u/γ. For relativistic electrons the wave is essentially indistinguishable from a true plane wave. Radiation scattered from the traveling wave in the $+Z$-direction has a wavelength $(\lambda_u/\gamma) + 2\lambda_C$, where λ_C is the Compton wavelength (h/mc). This scattered wave is the one emitted by the free electron laser, and its shift is due to the recoil of the electron. Similar considerations apply for absorption with emission and absorption in this geometry differing in wavelength by four Compton wavelengths.

The separation in frequency of stimulated emission and absorption is basically an interference effect. The amplitude for emission of radiation by an electron is the coherent sum of emission amplitudes at each point along its trajectory in the magnetic field. The same is true for absorption, and the total sum is nonzero only for wavelengths in which each term has similar phase. Such constructive interference in the periodic wiggler field (λ_u) gives a wavelength of emission:

$$\lambda \approx \frac{\lambda_u}{2\gamma^2}\left[1 + \left(\frac{1}{2\pi}\right)^2 \frac{\lambda_u^2 r_0 B^2}{mc^2}\right], \quad (1)$$

where r_0 is the classical electron radius and B is the magnetic field strength (Elias *et al.* 1976).

Laboratory experiments show that large gains are possible in free electron lasers (Elias *et al.* 1976; Attwood, Halbach, and Kim 1985); the maximum theoretical gain for a broad beam is

$$G \propto \lambda^{3/2}\lambda_u^{3/2} B^2 n_b \left(\frac{\Delta\nu}{\nu}\right)^{-2}, \quad (2)$$

where n_b is the electron beam density, $\Delta\nu$ is the emission-line width, and ν is the operating frequency (Hz). As is seen from relation (2), the maximum gain is essentially linear in electron beam current and quadratic in magnetic field strength. For such systems, "efficiency" is defined as the fraction of the original electron beam energy that can be extracted as electromagnetic wave energy. Early results for free electron laser configurations (Elias *et al.* 1976) showed electromagnetic wave generation efficiencies of $\sim 5\%$; more optimized modern configurations can achieve efficiences of 10%–20%, or more.

ii) *Relativistic Electron Beams Interacting with Plasmas*

In a laboratory experiment pertinent to astrophysical jet emission, strong, broad-band microwave emission has been observed when a relativistic electron beam penetrates an ambient thermal plasma (Kato, Benford, and Tzach 1983). In these experiments, an annular relativistic electron beam ($E \sim 1$ MeV) traverses an unmagnetized or weakly magnetized plasma column, where beam densities of $1\%-\sim 100\%$ of the background plasma have been used. Total emitted powers exceeding 20 MW are observed across a bandwidth of ~ 40 GHz (above ~ 10 GHz).

To account for this, Kato, Benford, and Tzach (1983) invoke a model in which the incident relativistic electron beam produces large-amplitude electrostatic waves in the background plasma. They argue that the beam electrons effectively collide in a coherent fashion with the electrostatic waves driven by the beam-plasma instability. All electrons within a single bunch move in phase, and the wave-particle interaction boosts the electrostatic wave up in frequency by the Compton effect (see Windsor and Kellogg 1974). Whereas single-particle power generated in these experiments is ~ 1 W, the observed coherent emission process produces power $\gtrsim 10^6$ times higher.

Kato, Benford, and Tzach (1983) estimate that in their laboratory configuration some 10^{12} beam electrons lie within the volume (λ^3) determined by the electrostatic wiggler wavelength $\lambda \sim v_b/\nu_{pe}$, where the beam velocity is $v_b \sim c$ and the plasma frequency in their case is $\nu_{pe} = \omega_{pe}/2\pi \gtrsim 10$ GHz. As will be discussed below, the relativistic effects boost the radiation into an emission frequency $\sim\gamma^2\nu_{pe}$. The electromagnetic power in these experiments emerges within an angle $\sim\gamma^{-1}$ of the beam direction, as expected from the Compton boosting mechanism. For relatively high beam densities, the emitted power is completely dominated by broad-band emission rather than by power at discrete harmonics of the plasma frequency. It is believed that a broad spectrum of electrostatic waves is driven by the higher density beams, and the Compton scattering of this spectrum off the relativistic electrons produces the observed frequency spread of the emitted radiation. In § III, we will develop further a model of Langmuir turbulence which is relevant to the relativistic electron beam–plasma interaction case.

As is evident from the above description, there is a strong analogy between the free electron laser and the relativistic electron beam–plasma interaction. In the latter case the wiggler field is produced by a beam-plasma instability. In both cases, one is able to produce extremely high emitted powers in the forward (beam) direction by means of a collective, coherent stimulated emission process. Such "masing" effects clearly overwhelm incoherent synchrotron emissions as arise from single-particle motion.

III. AN INNER JET MODEL BASED ON COHERENT EMISSION

Based on laboratory and space plasma physics experience, we feel that it is important to consider the possibility that partially coherent, highly directional stimulated emission is being produced in astrophysical jets. The amplification of stimulated emission may be a significant or even dominant source of emission in many jets if magnetic field geometries are proper and if plasma instabilities are driven within the jets by relativistic electron beams. We explore these features in this section, where a model for electromagnetic wave emission near the base of a jet is developed.

We next consider the stimulated emission of coherent radiation as a two-part mechanism. First, we assume that a relativistic electron beam passes through the jet plasma: this gives rise to Langmuir wave turbulence via a beam-plasma instability. Consistent with beam driving of Langmuir waves, the beam electrons will become charge bunched. Second, we consider the collective radiation of electromagnetic waves from these charge-bunched electrons passing through the Langmuir wave turbulence.

Although a variety of electrostatic instabilities feed on the drift velocity of electrons, there is considerable evidence that waves which are uncorrelated at low amplitude eventually form into localized knots of high-level wave turbulence. The phenomenon of "caviton collapse" was predicted by Zakharov (1972) and has spawned a wide literature which strongly supports the view that no matter what the details of birth, electrostatic turbulence forms a final end state of intense, compact electric field structures. "Strong" turbulence occurs when $W = \langle E^2\rangle/4\pi nkT > (k_0\lambda_D)^2$ and evolves to shorter

© American Astronomical Society • Provided by the NASA Astrophysics Data System

1988ApJ...326..110B

wavelengths as W increases. There are many unanswered questions about details of the strong regime, but numerical simulations show strong dissipation into heating of background electrons and ions (Goldman 1984).

Recent experiments support the view of a steady state balance struck between incoming drift energy and dissipation into heating and electromagnetic radiation (Benford *et al.* 1986). Although there is apparently no formal steady state in which all time derivatives are zero, estimates of radiative efficiency $\sim 1\%$ per meter in laboratory beams agree qualitatively with experiment. Radiation emerges as long as the beam motion (current) persists. Recent Stark effect measurements show a steady state $P(E) \propto \exp(-E^2/E_0^2)$, with $E_0 = 85$ kV cm^{-1}, a very high field even for intense beam experiments (Levron, Benford, and Tzach 1987). These results came from warm beam experiments, and thus apply to more relaxed environments after some broadening of an initially cold beam has occurred, due to the turbulence itself. The usual picture of an initially cold beam scattered and warmed by its self-induced electric fields seems to yield a persistent state in which cascade of electrostatic wave energy from resonant waves at λ_0 down to $(k\lambda_D) \approx 0.1$ proceeds without long-term loss of electric field strength or halting of radiation.

We shall assume that the details of the initial instability will be swallowed up in the general phenomena of wave cascade and subsequent nonlinear stabilization by a variety of processes (Goldman 1984). These electrostatic processes do not interfere with the linear electromagnetic growth rates of fire hose instability, so we shall treat them separately.

The persistence of the electric field distributions and strengths found experimentally by Levron *et al.* suggest that we can envision the radiating region of a jet as a steady reservoir of electrostatic and electromagnetic emission. Local variations will be smoothed out by the spatial average. In the Levron *et al.* experiments, microwave emission appeared coincident with the beam current and ceased as the current ended, although there were signs that the electrostatic fields lasted for times far longer than given by conventional collapse times of strong turbulence. This suggests that collective emission demands both drifting electrons and strong electric fields, present simultaneously.

The gap region reflects low-amplitude, linear growth of the fire hose mode. In a steady situation, though, there seems some possibility that waves will reflect back into this zone and hasten or even damp growth. This seems unlikely given the strongly convective nature of these modes, but the unavoidable inhomogeneities and variations in the jet path make reflection modes significant. We shall assume that at worst they do not suppress wave growth along the jet, although they may affect calculated growth lengths.

a) Langmuir Wave Turbulence Length Scales

A Langmuir wave is an electrostatic plasma oscillation with a frequency near the plasma frequency, $\omega_{pe} = (4\pi n e^2/m_e)^{1/2}$. Langmuir waves are typically driven unstable by the passage of an electron beam through a plasma. If a relativistic electron beam passes through a background jet plasma with a higher density, then, in the jet (observer's) frame, a beam-driven Langmuir wave will satisfy

$$\frac{\omega}{k} \approx v_b \,, \tag{3}$$

and

$$\omega \approx \omega_{pe} \,, \tag{4}$$

where ω is the angular frequency of the Langmuir wave, $k = 2\pi/\lambda$ is its wavenumber in the plasma frame, v_b is the electron beam velocity, and ω_{pe} is the jet plasma frequency. The origin of conditions (3) and (4) lies in the fact that a two-stream instability is a coupling of a beam to a plasma via a wave, with both the beam and the plasma resonating with the Doppler-shifted wave at their respective plasma frequencies. Relation (4) follows, therefore, since the observer's frame is that of the jet plasma and $\omega = \omega_{pe}$ is the condition for resonance with this plasma. Equation (3) comes about because the wave must travel nearly at the speed of the beam so that the beam perceives the wave Doppler-shifted down to the (low) plasma frequency of the low-density beam which is well below that of the jet plasma. The Langmuir wavelength is $2\pi/k$, so that in the laboratory frame

$$\lambda \approx 2\pi \frac{v_b}{\omega_{pe}} \,. \tag{5}$$

In calculating the characteristics of the emitted electromagnetic waves later in this section, this wavelength will be considered as the typical wiggler wavelength.

In order to estimate the turn-on distance from the jet source for the anticipated electromagnetic wave emission, the distance required for the growth of Langmuir wave turbulence must be determined. To do this, a simple, one-dimensional, two-fluid theory is used here to calculate the linear growth phase of electrostatic waves when a cold, relativistic electron beam penetrates the assumed warm, nonrelativistic jet plasma. The warm jet plasma is taken to be at rest, and the relativistic beam is considered to be propagating parallel to a uniform magnetic field that points in the x-direction. Only planar Langmuir waves that propagate in the x-direction are considered. Since Langmuir waves are high-frequency oscillations, only the fluctuating charge densities of the beam electrons and of the jet electrons are considered (all ion motions are ignored). The theory follows § 6.6 of Chen (1984), except that the jet electrons are taken to be warm and the beam electrons are allowed to be relativistic. As in Chen's development, combining the two equations of motion for the beam electrons and the jet electrons, the two equations of continuity for the beam and the jet electrons, and Poisson's equation (which relates the space-charge densities of the beam electrons and jet electrons to an electrostatic field) with the assumption that all perturbed quantities vary as $e^{i(kx-\omega t)}$, the dispersion relation

$$1 = \frac{\omega_{pb}^2}{\gamma^3(\omega - kv_b)^2} + \frac{\omega_{pe}^2}{\omega^2 - 3k^2 v_{te}^2} \tag{6}$$

is obtained. Here $\omega_{pb} = (4\pi n_b e^2/m_e)^{1/2}$ is the electron plasma frequency of the relativistic beam in its own reference frame, $\omega_{pe} = (4\pi n_p e^2/m_e)^{1/2}$ is the electron plasma frequency of the jet plasma, and $v_{te} = (k_B T_e/m_e)^{1/2}$ is the electron thermal velocity of the jet plasma. Because plasma kinetic effects are ignored, dispersion relation (6) is only valid for waves with phase speeds much greater than v_{te}.

Appropriate to the boundary value problem of relativistic electrons being injected into the jet plasma from the core source, solutions to dispersion relation (6) with ω real and k complex are sought. We seek an unstable wave mode, one having an imaginary part of k that is negative, corresponding

© American Astronomical Society • Provided by the NASA Astrophysics Data System

1988ApJ...326..110B

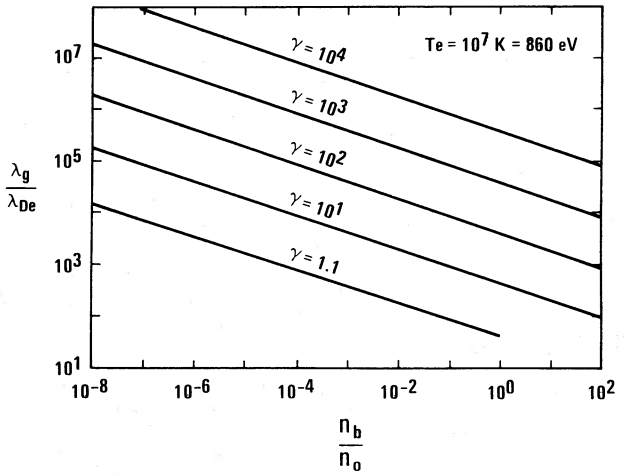

FIG. 3.—Growth length of Langmuir wave turbulence (in units of plasma Debye length) vs. relativistic electron beam density (in units of background plasma density). Growth scale lengths are presented for several different electron beam energies (γ) assuming an electron temperature of 10^7 K.

to exponential wave growth with distance from the source. For a given ω, such solutions are readily obtained by numerically solving equation (6), and the solution with the fastest growth is obtained by varying ω. Figure 3 plots the numerically obtained minimum required growth distances for the Langmuir turbulence (in units of the background plasma Debye length, $\lambda_{De} = 2.18 \times 10^4$ cm/$n_0^{1/2}$) versus relative beam density. In the calculations, we have assumed a jet plasma temperature of 10^7 K. Each curve corresponds to a different beam electron relativistic factor γ (i.e., beam energy). For an example, with $\gamma = 10$ and a relative beam density of 10^{-3}, the scale distance for Langmuir growth is $\lambda_g = n_0^{-1/2} 9 \times 10^7$ cm, where the background number density, n_0, is given in cm^{-3}. These growth lengths are sufficiently short with respect to the jet radius that the infinite plasma assumption taken in obtaining the dispersion relation (6) is justified. For For $\omega_{pb}^2/\gamma^3 \ll \omega_{pe}^2$, appropriate to a low density beam and/or a highly relativistic beam, the dispersion relation (6) can be solved analytically, yielding (in the background plasma frame) the growth length

$$\lambda_g = \frac{4\pi}{\sqrt{3}} \gamma \left(\frac{v_b}{v_{te}} \frac{n_0}{n_b}\right)^{1/3} \left(1 - 3\frac{v_{te}^2}{v_b^2}\right)^{1/2} \lambda_{De} \propto \gamma v_b^{1/3} T_e^{1/3} n_b^{-1/3} n_0^{-1/6} . \quad (7)$$

Note that if the relativistic electron beam is not cold, a kinetic theory that accounts for wave-particle resonances must be used in place of the fluid theory to calculate the growth length for the Langmuir wave turbulence. Within a distance of several growth lengths λ_g, the beam-driven Langmuir wave turbulence will be well developed, and a spectrum of Langmuir waves that propagate both parallel to and oblique to the beam will be present.

As each beam electron passes through the Langmuir wave turbulence, it encounters a spatially varying electrostatic field, causing it to oscillate and therefore radiate electromagnetic waves as in the free electron laser discussed in § II*b* above. Since $v_b \approx c$, an electron nearly keeps up with a forward-emitted electromagnetic wave in the rest frame of the jet; hence, forward-emitted waves are Doppler-shifted upward in frequency. Likewise, backward emitted waves are Doppler-shifted downward in frequency. Among other things, this leads to a strong forward beaming of the radiated power.

For a Langmuir wave with a wavelength of λ_0 forming the wiggler, the frequency of the emitted electromagnetic radiation is estimated as follows. From consideration of the wave and electron motion it is seen that $v_b t + \lambda_{em} = ct$, or, $\lambda_{em} = (c - v_b)t$, where λ_{em} is the wavelength of the forward-emitted electromagnetic wave and where t is the time (in the jet frame) that the electron takes to travel through λ_0. This time is $t = \lambda_0/v_b$, yielding

$$\lambda_{em} = \left(\frac{c}{v_b} - 1\right)\lambda_0 . \quad (8)$$

The relativistic factor for the beam is $\gamma = (1 - v_b^2/c^2)^{-1/2}$, giving $v_b/c = (1 - 1/\gamma^2)^{1/2}$. Thus equation (8) becomes

$$\lambda_{em} = \left[\left(1 - \frac{1}{\gamma^2}\right)^{-1/2} - 1\right]\lambda_0 . \quad (9)$$

For $\gamma \gg 1$, we recover (to lowest order) the relation for stimulated emission (eq. [1]) above:

$$\lambda_{em} \approx \frac{1}{2}\frac{1}{\gamma^2}\lambda_0 . \quad (10)$$

The frequency $\omega_{em} = 2\pi\nu_{em}$ of the forward-emitted electromagnetic wave is $\omega_{em} = 2\pi c/\lambda_{em}$. Using the beam-driven Langmuir wave of equation (5) for a typical wiggler and equation (8) for the wavelength boost gives

$$\omega_{em} \approx \frac{c}{c - v_b}\omega_{pe} \quad (11)$$

or, for $\gamma \gg 1$ (with eqs. [5] and [10])

$$\omega_{em} \approx 2\gamma^2\omega_{pe} , \quad (12)$$

where $v_b \approx c$ was used. This is an alternate description of the the so-called Compton boosting (Windsor and Kellogg 1974) of an electromagnetic wave by interaction with a Langmuir wave. It is a Doppler shift of the radiation from a moving oscillator. The Doppler shift factor of γ^2 is for emission in the forward direction. For emission of waves in the direction perpendicular to the beam velocity, there is no Doppler shift and the electromagnetic wave frequency is $\nu = 1/t$, where t is as defined earlier in this paragraph. Similarly, the frequency of a backward-emitted electromagnetic wave is Doppler downshifted in frequency from the plasma frequency ω_{pe}. Thus for a relativistic electron the power emitted is much greater in the forward direction than in other directions.

With the wiggler being a wave, the beam electron interacts with the collective field of all the jet plasma charged particles composing the wave; thus the acceleration of the electron is large, and the power emitted is great because the power is proportional to the square of the magnitude of the acceleration. Another factor that greatly enhances the power emitted is the fact that the beam electrons are resonating with the Langmuir wave and are therefore themselves charge bunched. (The Langmuir waves actually being space-charge patterns, the growth length of the Langmuir wave is the growth length of the charge bunching.) Thus, the electromagnetic emission is the result of coherent radiation from large numbers of beam electrons oscillating in phase. The power emitted is proportional to $Q^2 = N^2e^2$, where Q is the charge in one clump on the beam, N is the number of electrons in a clump, and e is the electronic

© American Astronomical Society • Provided by the NASA Astrophysics Data System

1988ApJ...326..110B

charge. For a beam with a density n_b lower than that of the plasma n_0, an upper limit to the number of beam electrons in a clump is given by $N \sim n_b \lambda^3$, yielding, with relation (5) and with $v_b \approx c$,

$$N \sim 3.7 \times 10^{19} \frac{n_b}{n_0^{3/2}}, \quad (13)$$

where n_b and n_0 are in cm^{-3}.

To obtain an estimate of the power emitted by the beam-driven plasma, the theory of Kato, Benford, and Tzach (1983) can be generalized to the radio jet case, or an upper limit to the power emitted can be obtained from first principles. Such a first principles upper limit is developed in Appendix A, resulting in the expression

$$P = 3.6 \times 10^{-5} \text{ ergs s}^{-1} \left(\frac{n_0}{\text{cm}^{-3}}\right)^{3/2} \left(\gamma \frac{\delta n}{n_0}\right)^4 f V_{\text{plasma}} \quad (14)$$

for the maximum power emitted by the plasma, where n_0 is the number density of the plasma, γ is the relativistic factor of the driving electron beam, δn is the amplitude of the number density modulation of the plasma (or beam), f is the filling factor of the beam-driven Langmuir waves, and V_{plasma} is the volume of the plasma. As an example, an $n_0 = 10^{-3}$ cm^{-3} density plasma with a volume of 1 kpc^3 driven by a $\gamma = 10^4$ beam such that $\delta n/n_0 = 10^{-1}$ will emit 10^{41} ergs s^{-1} of radio emission at a characteristic frequency of 2.8×10^{10} Hz if the filling factor of the clumps is $f = 2.7 \times 10^{-27}$. Note, however, that the relation between the power emitted by the plasma and the filling factor is extremely sensitive to γ and to $\delta n/n_0$. Since the emission from radio sources is quite inhomogeneous, the radio source plasmas are probably very inhomogeneous and may have small, possibly transient regions where conditions permit clumping. These regions would dominate the flux density within a synthesized beamwidth and could account for essentially all of the emission.

A similarity between the Compton-boosted mechanism and the synchrotron mechanism lies in the fact that the Compton-boosted emission peaks at a frequency of $\gamma^2 \omega_{\text{pe}}$, while synchrotron radiation peaks at $\gamma^2 \omega_{\text{ce}}$, and for standard jet parameters these are nearly the same (i.e., $\omega_{\text{pe}}/\omega_{\text{ce}} = 0.3 n_{-4}^{1/2}/B_{-4}$). As argued by Benford (1985), the polarization and other spectral features are indistinguishable between the two mechanisms, if we make the customary assumptions of isotropic particle distributions with a power law in energy. To contrast this collective emission mechanism with the single-particle synchrotron emission mechanism, the power gain G of the coherent plasma process over that of the incoherent synchrotron radiation is estimated here. The total power output of the plasma is amplified for the coherent case by the factor

$$G = \frac{\langle E^2 \rangle}{B^2} \frac{N^2 N^*}{N_e}, \quad (15)$$

where $\langle E^2 \rangle$ is the average squared electric field of the electrostatic turbulence, B is the magnetic field strength, N is the number of electrons in a clump, N^* is the number of clumps, and N_e is the number of electrons. The turbulent electric field E can be much smaller than the ambient field B and still G can be very large, since the N^2 factor can be so dominating. In like fashion, the lifetime of a radiating electron is reduced by G^{-1}, imposing further constraints on the distance within which electrons must be reaccelerated in jets. However, an electron will generate incoherent synchrotron radiation wherever it encounters a magnetic field at a significant pitch angle, but conditions for coherent radiation may be transient. Thus, the ratio of lifetimes if the radiation is collective to the radiation being synchrotron is proportional to f/G. With f being small, an individual particle may propagate a great distance without encountering a coherent region. When it does, it will emit energy that was gained at a reacceleration site far removed.

Large gains, $G \gg 1$, imply that much less energy needs to be tied up in a jet in order to yield its observed power emission; typically, $\sim G^{-1}$ of the usual estimated energy density. We are extrapolating from experiments at high-energy density to low-energy density astrophysical environments. The contrast is $\sim 10^4$ in γ, 10^{14} in N (independent of n_b/n_0), and $\sim 10^{-24}$ in f. Power is affected by $N^2 f$, however, which need change by only 10^4 to explain observed astrophysical emission. We are relying on only a few points of fundamental physics. We use the fact that a beam electron passing over a plasma wave charge clump of size a emits frequencies $\omega \approx 2\gamma^2 c/a$, and that some beam clumping results, to give coherent radiation. These features should apply no matter what the numerical range of parameters. Further, we need only an astonishingly small f to yield the observed power, so the right turbulence conditions can be rare indeed. Lastly, the laboratory experiments cited can simulate the Type III solar burst phenomena (e.g., Goldstein, Smith, and Papadopoulos 1979), a scaling in distance of 10^{11}. The underlying physics—beam-plasma turbulence, mode coupling versus quasilinear formation and subsequent emission—applies on both scales. This reassures us that such extrapolation has meaning and can be predictive.

In this collective emission process, the electron clumps radiate when they experience transverse velocity kicks. Therefore, in addition to suffering a radiative energy loss while they are within the coherent zones of the plasma, the electrons also experience a pitch-angle scattering. Accordingly, the more radiation that is emitted from the plasma, the more pitch-angle scattering there is of the beam electrons. The isotropization time for this process is experimentally estimated as (from eq. [5] of Baranga, Benford, and Tzach 1985)

$$t \sim 4.4 \times 10^{-8} \text{ s} \frac{1}{f} \frac{n^{1/2}}{\gamma^{3/2}}, \quad (16)$$

where n is in cm^{-3}. As was the case for the radiated power output from the plasma, the pitch-angle scattering time is very sensitive to the filling factor f. For the $f = 2.7 \times 10^{-27}$, $\gamma = 10^4$, $n_0 = 10^{-3}$ cm^{-3} example used earlier in this section, the Langmuir wave scattering time for the electrons is $t \sim 1.6 \times 10^4$ yr. For a jet, as the electron beam propagates out from the central engine, it will broaden in velocity space as it radiates. Accordingly, the beam will be coolest nearest the core, and, owing to the fluid-like nature of the instability and the resulting stronger beam bunching, the radiation will probably be most intense there. Further from the core, the beam will be warmer, the instability will be kinetic rather than fluid-like, the bunching will be weaker, and the emissivity of the plasma probably will be lower. This pitch-angle scattering of the beam also has implications for the growth of the fire hose instability discussed in the next subsection.

b) Relativistic Beam–driven Fire Hose Instability Length Scales

In addition to the short-wavelength electrostatic waves that act as the wiggler field, we also expect very long wavelength

© American Astronomical Society • Provided by the NASA Astrophysics Data System

1988ApJ...326..110B

electromagnetic waves to arise further down the jet. These long-wavelength electromagnetic instabilities are of interest here because they may act to point the beamed electromagnetic wave emission in random directions, making the jet visible to observers whose lines of sight are not aligned with the jet's axis. There exist several candidate mechanisms for producing such low-frequency electromagnetic plasma waves: the more common instabilities are the kink, the Kelvin-Helmholtz, and the fire hose. The kink instability is driven by a magnetic field–aligned current flowing within the plasma; the long-time evolution of this instability results in a coiling up of the magnetized current filaments (Dattner 1962). However, unless the current carried by the jet is highly filamentary, this instability can be ruled out, since only wavelengths that are long compared with the size of the current channel (jet) are unstable (Gary, Gerwin, and Forslund 1976). The Kelvin-Helmholtz instability can be driven by a beam of electrons that has a radial dependence in kinetic energy. The long-time evolution of the Kelvin-Helmholtz instability results in the production of plasma vortices, in the driving of low-frequency compressive electromagnetic plasma waves, and in a turbulent behavior of the plasma (Kivelson and Pu 1984; Birn *et al.* 1985). Because the Kelvin-Helmholtz instability is inherent to inhomogeneous plasmas, an eigenvalue problem must be solved particular to the jet geometry in order to obtain its growth rate. The nature of this problem depends strongly on the model taken for the magnetic field geometry and the plasma inhomogeneity, and the result depends strongly upon the nature of the boundary layer formed between the jet plasma and the ambient plasma. For the calculation of instabilities, a further complication is that the boundary layer does not form axisymmetrically around the jets. The formation of plasma boundary layers around extragalactic jets will be discussed in a future report.

The last of the candidate instabilities mentioned above is the fire hose (Noerdlinger 1968; Noerdlinger and Yui 1969). In its linear stages, a fire hose instability is manifested in Alfvén waves of near-zero frequency in which the ambient magnetic field veers sinusoidally in direction. In its nonlinear stages (further from the source), the fire hose leads to a snarling and jumbling of the magnetic field lines in the plasma, possibly accompanied by plasma compressions. The fire hose instability is driven by a pressure anisotropy in a magnetized plasma such that

$$P_{\parallel} - P_{\perp} > \frac{B^2}{8\pi} . \tag{17}$$

The pressure ($P_{\parallel}$) parallel to $\boldsymbol{B}$ is the ram pressure of the relativistic beam, plus the ram pressure of the plasma outflow, plus any thermal pressure of the plasma and the beam. The pressure ($P_{\perp}$) perpendicular to $\boldsymbol{B}$ is the magnetic field pressure $B^2/8\pi$ plus any plasma or beam thermal pressure. As a lower limit to the growth length of the fire hose mode, the instability driven by an absolutely cold relativistic electron beam will be considered. As an upper limit to the growth length of the fire hose mode, the minimum electron pressure anisotropy produced by synchrotron loss will be considered.

The cold beam–driven fire hose is considered first. Using a normal-mode analysis of Maxwell's equations with cold plasma source terms, a dispersion relation for the jet plasma is obtained in Appendix B (see eq. [B1]) and this dispersion relation is numerically solved and the solutions are displayed in Figure 6. As can be seen, the growth of the fire hose instability is remarkably rapid, growth lengths of 100 pc being typical, although these growth lengths would be considerably longer if finite-plasma boundary effects would be included.

For the upper limit to the growth length of the fire hose mode, a minimum anisotropy for the relativistic electrons consistent with single-particle synchrotron energy loss can be determined. The basis for this limit is that even for an initially isotropic distribution, an isotropy will arise in a finite amount of time via synchrotron losses. This anisotropy leads to the growth of the fire hose mode, which in its nonlinear stages will act back on the anisotropic electron distribution to isotropize it. As an estimate of the time for the synchrotron cooling of an initially isotropic distribution of relativistic electrons to develop sufficiently large values of $P_{\parallel}$ relative to $P_{\perp}$ such that condition (17) is satisfied, the synchrotron decay time for a 90° pitch-angle electron is used (Alfvén and Fälthammar 1963)

$$t = \frac{3m_e^3c^5}{2e^4\gamma B^2} = 2.1 \times 10^8 \text{ s } \frac{1}{\gamma B^2} , \tag{18}$$

where B is in gauss. The upper limit to the growth length L of the fire hose instability is then approximately the net electron drift velocity v_{drift} multiplied by this growth time. As one estimate for the electron drift velocity, the drift of a velocity-space hemisphere of relativistic electrons is taken, $v_{\text{drift}} = 4c/3\pi$. This yields the upper limit

$$L \sim 0.87 \text{ pc } \frac{1}{\gamma B^2} .$$

As another estimate of the electron drift velocity, the ion-acoustic speed maximized to a 100% relativistic electron plasma is used, $C_{s_{\max}} = 7.0 \times 10^8$ cm s$^{-1}\gamma^{1/2}$. This yields the upper limit

$$L \sim 4.8 \times 10^{-2} \text{ pc } \frac{1}{\gamma^{1/2}B^2} . \tag{20}$$

If it is assumed that $B = 10^{-4}$ G and if $\gamma = 10$, then equations (19) and (20) yield the upper limits to the fire hose growth length 8.7 and 1.5 Mpc. Thus the synchrotron cooling limit to the fire hose growth is not at all restrictive.

The upper and lower limits to the fire hose growth length serve to bracket the growth length only very weakly, from $\sim$100 pc to $\sim$20 Mpc. Unfortunately, a proper calculation of the beam-driven fire hose instability would require a complete modeling of the core, jet, and ambient media. Thus, a two-outflow (bulk plasma plus electron beam) core model must be constructed to obtain the phase-space distribution functions $f(\boldsymbol{v}, \boldsymbol{r})$ of the outflowing particles. Because such a calculation is not provided in this report, we can only suggest that the gap turn-on is caused by the onset of long-wavelength electromagnetic plasma modes.

Because the amplitude of the spatially growing low-frequency waves is exponential with distance along the jet, the waves will suddenly appear above threshold. Their presence will be noted as even more sudden by an oblique observer, since the radiation from the jet can be detected only at a low level until the low-frequency waves are of large amplitude. This apparent rapid onset is characteristic of wave growth with distance from a stabilizing boundary, as can be seen in the figures of Dattner (1962), in Figure 2 of Elder (1960), in Plate 1*a* of Polymeropoulos and Gebhart (1967), and in

© American Astronomical Society • Provided by the NASA Astrophysics Data System

1988ApJ...326..110B

Figure 1 of Jones, Lemons, and Mostrom (1983). This rapid onset, in connection with the forward beaming of the Langmuir-wave–induced electromagnetic wave radiation, we hypothesize as the origin of the gap turn-on of jet emission. In our model, the turn-on point denotes a region of the jet where the waves have grown to an amplitude such that $\Delta B/B \sim 1$, where ΔB is the wave magnetic field amplitude and B is the ambient magnetic field strength. Thus, at the turn-on point, the waves are of nonlinear amplitudes, and beyond the gap the magnetic field is expected to be turbulent-like with an underlying magnetic field direction, much like the solar wind.

c) *An Overview of the Inner Jet Model*

With the above estimates and plasma physical ideas in mind, we present our model of jet emission and inner jet structure.

We consider an extragalactic or stellar jet system with a central core region and relatively linear jet structures (either double or single sided). These jet structures commonly end in large radio lobes. Figure 4 shows a significant luminosity gap (Bridle and Perley 1984), which in the extragalactic jet case can be many kiloparsecs in size. We assume that jets are nonrelativistic plasma flows that emanate from the central core and that may contain entrained intergalactic plasma. We also assume that, near the core, the jets contain axially aligned magnetic field lines carried with the bulk plasma flow. Superposed on this low-velocity plasma and field structure, we assume a highly beamed relativistic electron population streaming outward along the jet axis (parallel to $\boldsymbol{B}$) from the central engine. Thus, we assume that a low-velocity plasma flow determines the overall source dynamics, maintaining an axial magnetic field in the jet and supplying matter and energy to the extended source. We postulate that, at least in the nuclear region, the core of this jet is penetrated by a directed, relativistic electron beam. This beam could arise, for instance, from a region similar to that described by Lovelace (1976), with a scale size of 10^{16}–10^{17} cm within which positron-electron annihilation cascading in a region of strong electric and magnetic fields eventually produces an intense directed beam of high-energy ($\gamma \gtrsim 10$) electrons.

A relatively short distance away from the core, we expect the relativistic electrons to produce Langmuir-wave turbulence (§ III*a*). Although a very wide range of jet parameters is possible, we expect (Fig. 3) Langmuir turbulence will be fully developed on a length scale λ_g somewhat greater than 1–100 AU, as illustrated in the lower part of Figure 4. Therefore, beyond a few λ_g, we surmise that relativistic electrons will pass through a Langmuir turbulence wave field of wavelength λ_L that they drive, causing a collective emission of electromagnetic radiation. This partially coherent emission will be strongly forward-beamed into a relativistic emission cone of angular width $1/\gamma$, with characteristic electromagnetic frequency $\omega \approx \gamma^2\omega_{pe}$. Unless an external observer is in the jet emission cone, he will see only incoherent synchrotron radiation from the relativistic electrons, and this will be relatively weak due to the

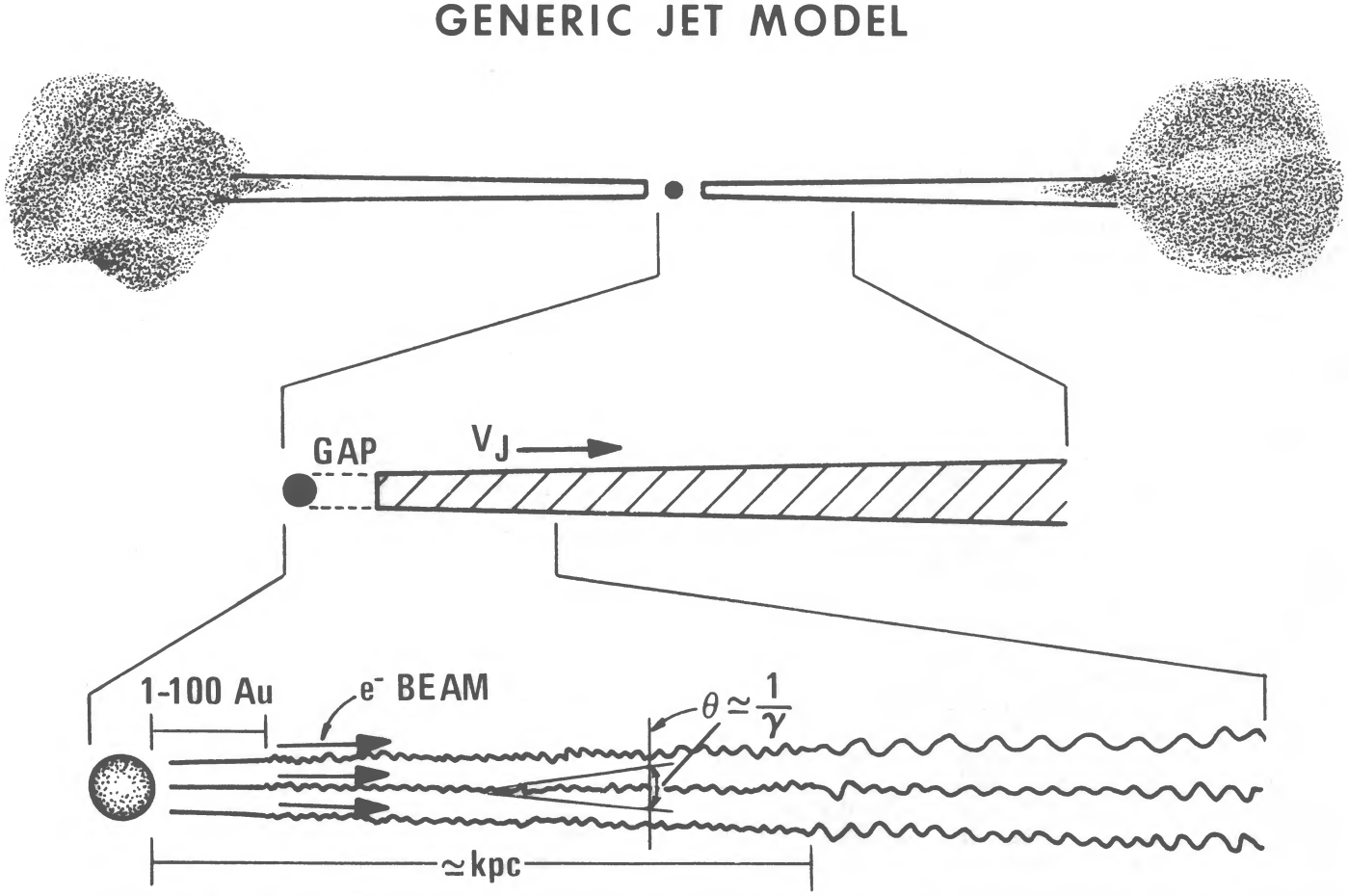

FIG. 4.—Schematic illustration of the morphological structure of an astrophysical jet showing details predicted by the model developed in this paper

© American Astronomical Society • Provided by the NASA Astrophysics Data System

1988ApJ...326..110B

highly beamed (field-aligned) character of this population. An observer within the emission cone would see powerful, Compton-boosted emission, and would interpret this signal as a BL Lacertae object.

On a greater scale length we expect the development of much longer wavelength instabilities. An obvious candidate, which was discussed above, is the fire hose instability. Another is the Kelvin-Helmholtz instability arising from the velocity shear of the jet flow through the ambient medium, or from a radially dependent profile of the relativistic electron beam. At any rate, on a scale length of 100 pc to Mpc we expect large-amplitude long-wavelength fluctuations in the magnetic field direction, the amplitude of the fluctuations increasing away from the core. Leaving the core source, the magnetic field lines will first begin to deviate slightly and later to snarl. These field lines will guide the relativistic beam electrons, which will continue to collectively emit electromagnetic waves in their forward direction. With onset of the large-scale magnetic field fluctuations, there begins to be a significant probability of the field lines making large angles with the jet axis. This random turning of the directions of the field lines will beam emission from the various flux tubes. Wherever this occurs, an arbitrarily located observer will be able to see the beamed emission arising from beam-plasma interactions. With relatively sudden onset of this disruptive behavior along the jet, the external observer will see a sharp brightening of emission because a fraction of the flux tubes with their beamed emission is pointing at large angles to the jet axis.

As shown by the lower portion of Figure 4, the sequence we have described above provides a natural explanation of BL Lacertae objects and of the luminosity gaps in galactic and extragalactic jets.

IV. PREDICTIONS OF THE MODEL AND DISCUSSION

Our model of astrophysical jets (Fig. 4) has several useful explanatory features and makes some testable predictions. Awaiting a fully quantitative model, we consider qualitative roles of coherent, stimulated emission in jets, which can profoundly effect the parameters and energetics of the jets themselves.

Many jets have radio-dim regions between the central core and the beginning of a visible jet (Bridle and Perley 1984). Such gaps are a natural consequence of coherent, highly beamed radio emission. We suggest that strong emission actually occurs all along the jet, and the emission near the core is nearly undetectable to an observer who is not in the beaming direction. For such an observer, the detectable emission from the gap region is weak, incoherent synchrotron radiation plus some beam-driven collective radiation with $\omega \ll \gamma^2 \omega_{pe}$. An intense, abrupt onset in detectable emission should occur when large-amplitude long-wavelength fluctuations arise, for example, from the relativistic fire hose or Kelvin-Helmholtz instabilities.

An observer lying within $\vartheta \sim 1/\gamma$ of the jet direction will see the full strength of the Compton-boosted stimulated emission from near the core. Relatively weak jets, when viewed from a large angle to the axis, would by virtue of the coherent beaming mechanism appear very bright when seen end-on. An observer would see only a portion of the emission from the regions of the jet that are strongly affected by the long-wavelength instabilities; hence, these regions would be considerably dimmer than the inner regions. The electromagnetic emission from a spiraling jet (see Fig. 5) would, in our model, show relatively bright regions at the edges of the spiral due to the coherent mechanisms. This is expected to contrast with regions of maximum brightness in the single-particle synchrotron model.

Thus, our model predicts that all radio sources have some relativistic beaming and Doppler boosting. The statistical predictions of the model, in terms of compact versus extended sources, or radio-strong versus radio-quiet sources, should be similar to those of the standard models which assume relativistic bulk flow (e.g., Kellerman 1985). Our model will differ slightly, in that the Doppler factor is higher, $\gamma > 10$, and in that some nonbeamed, incoherent synchrotron emission is also present. However, since the interpretation of the statistics in terms of beaming is still uncertain and model dependent (e.g., Peacock, Miller, and Longair 1986; Browne and Perley 1986; see also Owen 1986), we do not pursue this subject further.

In our collective emission model, electromagnetic polarization arises from an anisotropy in the electric field spectrum of the Langmuir turbulence. This anisotropy arises from two sources: the preferred direction of the relativistic electron beam that drives the waves and the ambient magnetic field. We expect that cold beams will drive Langmuir waves with electric fields aligned with the beam, and warm beams drive Langmuir waves with electric field vectors oblique to the beam. Details depend on the plasma and beam distribution functions $f(\boldsymbol{v})$ and upon $\boldsymbol{B}$.

Owing to the inherent anisotropy of the magnetized media, anisotropic electrostatic electron cyclotron wave turbulence may occur rather than Langmuir wave turbulence. The properties of the electrostatic electron cyclotron turbulence are not known since no fully developed turbulence has been observed, for example, in the solar wind (S. Fuselier 1986, private communication). Hence, we cannot currently estimate whether the electric field vectors will be aligned with or normal to the ambient magnetic field direction. Regardless of the preferred direction for the electrostatic wave, electric field vectors, polarization will be low when the jet is viewed end-on because the directions of the electric field vectors of the electromagnetic waves will average out, and polarization will be higher when viewed oblique to the jet axis. As is the radiation mechanism itself, the polarization is the same as that of relativistic bremsstrahlung (Lichtenberg, Przybylski, and Scheer 1975). Unless the electrostatic waves have their electric field vectors completely aligned with the beam, radiation is dominated by perpendicular accelerations of the beam clumps and emission is strongly linearly polarized with electric field vectors perpendicular to the beam direction. For small-angle deflections of the clump, the level of polarization of radiation directed along the beam is 0%, and for radiation on the edge of the $1/\gamma$ cone of emission the level of polarization is 100%.

If the relativistic electron beam is cold, the two-stream instability is fluid-like and all beam particles partake in the charge bunching, radiate collectively, and lose kinetic energy via this radiation. The γ-value of the beam falls as it propagates along the jet, decreasing $\gamma^2 \omega_{pe}$. As in synchrotron radiation, this appears as a spectral cooling with distance from the core. For warm beams, the two-stream instability is kinetic and only the portions of the beam in Landau (or cyclotron) resonance with the driven waves will bunch. They will radiate collectively, while the other beam electrons radiate incoherently as they pass through the turbulence. The most unstable portions of the beam will bunch and radiate the strongest, losing energy at a much higher rate. This randomizes the beam, lowering γ in the

© American Astronomical Society • Provided by the NASA Astrophysics Data System

1988ApJ...326..110B

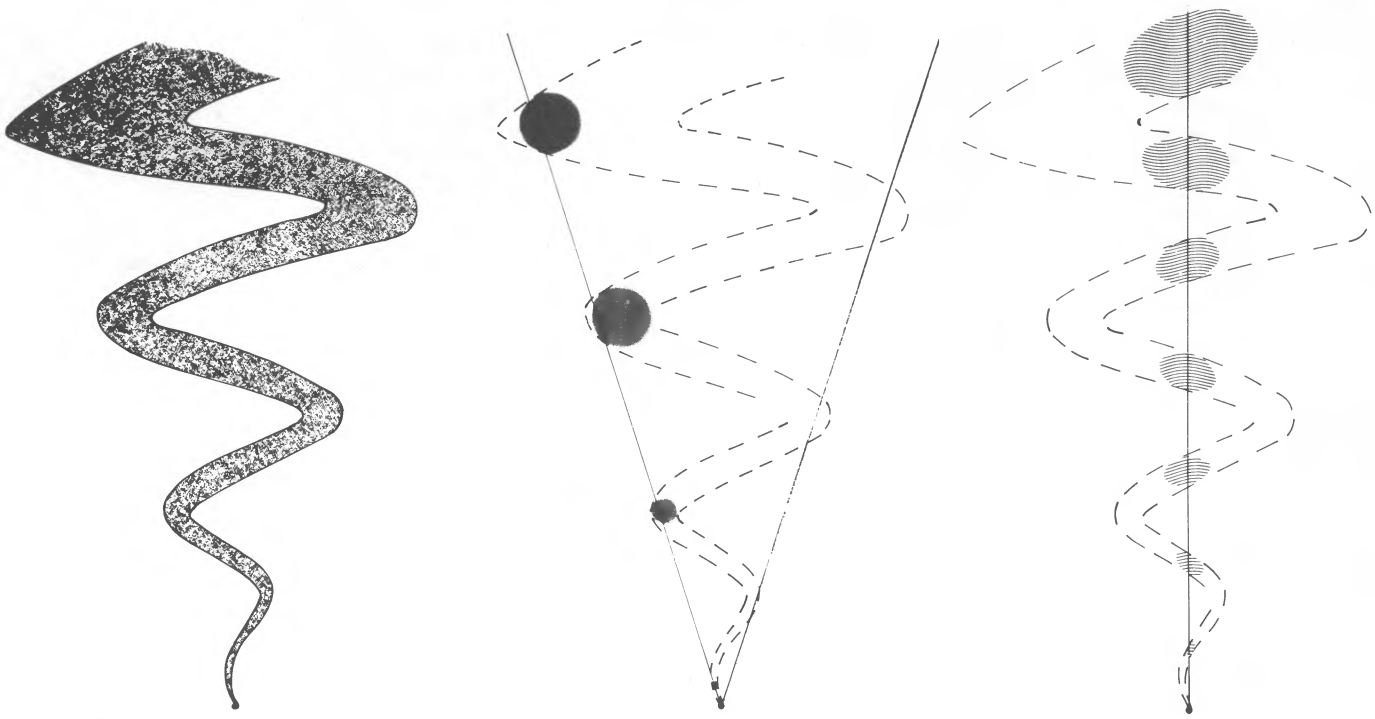

FIG. 5.—Plasma of a spiraling jet (*left*) as in SS 433. The electromagnetic emission from such a spiraling jet if the radiation is Langmuir wave–induced by an electron beam that spirals down the jet (*middle*). Finally, the emission if the radiation is single-particle synchrotron radiation (*right*).

region of resonance. Again this leads to a spectral cooling with distance along the jet. If only a small fraction of the beam radiates coherently, most of the relativistic electrons can travel the full length of the jet without any significant energy loss. This may lengthen electron lifetimes and reduce the need for in situ reacceleration in some sources (see also Spangler 1979).

If the relativistic electrons of the beam that drive the turbulence are too few in number to power the entire jet-lobe system, but only the inner jet radiation, then the model of this report is still compatible with the standard pictures of jet-lobe energy transport: kinetic energy flows (Blandford and Rees 1974) and electrical currents (Alfvén 1978; Benford 1978). Collective emission processes are unaltered by bulk outflows of the jet plasmas, provided that the flows are nonrelativistic; if they are relativistic, an additional Doppler shift of the emission occurs. Thus, kinetic energy can be carried past the inner portion of the jet via a plasma flow without invalidating the collective emission model applied there. Likewise an electrical current can be carried by a relative drift of the bulk-plasma electrons and ions without altering the electromagnetic wave emission. Accordingly, energy can be carried via a current through the inner jet without invalidating the collective emission model. The plasma outflow and/or the electric current do, however, have profound effects on the long-wavelength electromagnetic instabilities discussed in connection with the gap turn-on. The bulk outflow presents a source of ram pressure down the axis of the jet and the current produces magnetic shear around the jet azimuth, both greatly affecting the growth lengths of the fire hose and Kelvin-Helmholtz instabilities.

An issue of paramount importance in, and near, the core regions of jets concerns rapid radio flux variations and high brightness temperatures. As first discussed by Kellerman and Pauliny-Toth (1969), within the standard incoherent synchrotron picture there is a maximum brightness temperature $T_{\max}$ permitted for a radio source. Above $T_{\max} \sim 10^{11}$–10^{12} K, the density of required synchrotron-emitting electrons becomes so high that inverse-Compton scattering increases dramatically. This process boosts the synchrotron radiation into the X-ray range and causes such intense emission as to deplete the available electron free energy rapidly. When $T_{\max}$ exceeds 10^{12} K, inverse-Compton scattering becomes catastrophic and source brightness temperatures then decrease rapidly to values below 10^{12} K where synchrotron emissions are comparable to the Compton mechanism.

Still the fact that no observed sources give $T_{\max}$ exceeding 10^{12} remains the strongest argument for incoherent emission. Coherent processes can mimic this limit through a small packing fraction, so the spatially and temporally averaged brightness temperature $T_{\rm coh}$ is diluted by the packing fraction, f, and $T_b = fT_{\rm coh}$. With f very small, as argued below equation (14), many sources could have T_b well below 10^{12}, and the few sources which press this limit may indeed be incoherent emitters. The issue may then be not why no sources exceed 10^{12} but why so many sources (perhaps coherent) fall well below it. The answer is that coherent regions are rare, but nonetheless dominate the emission.

The phenomenon of radio "flicker" (Heeschen 1982; Simonetti, Cordes, and Heeschen 1985) suggests intrinsic time varia-

© American Astronomical Society • Provided by the NASA Astrophysics Data System

1988ApJ...326..110B

tions of compact sources in 1 or 2 days to perhaps 20 days. Spatial scale sizes consistent with such variations imply surface brightness temperatures greatly exceeding the 10^{12} K inverse-Compton limit for an incoherent synchrotron source. To reconcile these flicker results with the standard emission mechanism requires $\gamma_{\rm bulk} \sim 7$. Our model relying on coherent stimulated emission requires no relativistic bulk plasma motion and can explain observed ratio emissions with a $\gamma \sim 10$ electron beam population $\sim G^{-1}$ times less dense than the bulk flow, and with no ion flow.

In our model, flickering can come from three causes: (1) the relativistic electron beam may be modulated by the core source, (2) local conditions for coherent emission may be transient and hot spots may turn on and off, or (3) the long-wavelength low-frequency instabilities that steer the field lines may lead to a temporal sweeping of a flux tube's beamed emission across the line of sight to the observer. Since the time scales for Langmuir processes are $t \sim 1/\omega_{\rm pe}$, which is very rapid, the observed 1–20 day flickering near the cores of extragalactic jets rules out cause (2). Because the onset of the low-frequency electromagnetic instabilities is far from the core source, the observed flickering near the core is probably not produced by cause (3) either, unless there exists a high-frequency fast-growing electromagnetic instability. Therefore, the radio flicker near the core probably comes from a modulation in the relativistic-electron output of the central engine. This modulation implies important properties of the central engine, such as the time scales of perturbations in accreting fluid flows or release of inductive electrical energy.

The temporal modulation caused by the veering of the magnetic flux tubes may be discernible as a scintillation at the gap turn-on point. At the edge of the turn-on, magnetic flux tubes begin to make excursions about the jet axis sufficient to point their beamed emission at an observer. Hence, at the very edge of the turn-on, a relatively small number of flux tubes are pointed at the observer. Discrete signals from the individual flux tubes may be detected as these flux tubes sweep across the observer's position. The periods τ of these scintillations may correspond to the periods of the relativistic electron–driven fire hose. This period is $\tau \gtrsim (L/c, 2\pi/\omega_{\rm ci})$, L being the spatial scale resolved, and $\omega_{\rm ci} = eB/m_i c$ is the jet ion gyrofrequency.

As an estimate of the time scale, $\tau = 2\pi/v_{\rm A} k$ can be taken, $v_{\rm A}$ being the Alfvén speed of the medium. For turn-on of an extragalactic jet resolved to $\sim$100 pc, with $B \sim 10^{-5}$, $n_j \sim 10^{-4}$ cm^{-3}, then $\tau \sim 4.5 \times 10^4$ yr for the flicker. Even if c is used in place of $v_{\rm A}$ and 10 pc used instead of 100 pc, the estimate $\tau \sim 33$ yr is obtained. Owing to the much higher resolution, a more promising value is obtained for a stellar jet; with a VLA resolution size of 0.024 pc and with $n = 10$ cm^{-3} and $B = 10^{-2}$ G (Hjellming and Johnson 1982), the estimate yields $\tau = 2\pi/v_{\rm A} k = 600$ days. With a VLB1 resolution of 10^4 pc, $\tau \sim 3$ days. Such a flicker may be observable and may test this gap–turn-on model for stellar jets.

As remarked for the growth rate estimates of the fire hose instability (§ III*b*), a great dilemma arises in applying plasma physics to astrophysics: to obtain growth rates for plasma waves requires the details of the phase-space distribution function $f(v)$ for all particle species of the plasma. Even in solar system plasmas, these distributions are often not known in sufficient detail for a proper calculation of wave growth. For astrophysics, the only escape from this dilemma comes when the instability is clearly in the fluid regime, as was assumed for the Langmuir wave calculation of § II*a*. Then the *linear* plasma wave dynamics can be correctly discerned. For the nonlinear regime, substantial progress must be made before wave-particle effects can be theoretically discerned with confidence.

If our model for radio emission from jets is correct to any significant degree, the "normal" incoherent synchrotron assumptions (e.g., Gould 1979) are not valid. Therefore, the values obtained for the relativistic electron spectrum, the electron density, the magnetic field strength, and related quantities made from traditional synchrotron theory are not correct. Thus we are faced with a further dilemma: if our model is correct, then all of the parameters within the standard range that we have used here for illustration may be incorrect. Accordingly, the radio data from jets would have to be reanalyzed in order to form a self-consistent collective emission model.

We thank Alan Bridle, Jack Burns, Richard Epstein, Steve Fuselier, Peter Gary, Galen Gisler, Chris Goertz, Robert Hjellming, Mike Jones, Alan Marsher, Peter Noerdlinger, Frazer Owen, Steve Shore, and Meg Urry for useful discussions concerning this paper. Work at Los Alamos was done under the auspices of the US Department of Energy with support from the Office of Basic Energy Sciences. G. B. was supported by the AFOSR. J. A. E. was supported by grants from NASA-Ames Cooperative Agreement NCC 2-634.

APPENDIX A

THE POWER EMITTED BY THE LANGMUIR WAVE–INDUCED WIGGLER

An upper limit to the electromagnetic wave power emitted by the Langmuir turbulence–induced process can be obtained by applying Larmor's formula to a charge clump in the beam passing a charge clump in the plasma. Before making this application, it must be noted that, for a two-stream instability, the amplitude of the density modulation of the beam is equal to the amplitude of the density modulation of the plasma electrons, $\delta n_b = \delta n_0 = \delta n$, and the wavelength of the beam density modulation is equal to the wavelength of the plasma–electron-density modulation $\lambda_b = \lambda_0 = \lambda$, where λ is the observed wavelength of the two-stream–driven electrostatic wave.

For a beam clump containing N electrons, Larmor's formula yields the power emitted by the clump as it is undergoing an acceleration,

$$P = \frac{2}{3}\frac{N^2 e^2}{c}\gamma^6[(\dot{\boldsymbol{\beta}})^2 - (\dot{\boldsymbol{\beta}} \times \boldsymbol{\beta})^2] , \tag{A1}$$

where $\boldsymbol{\beta} = v/c$. Taking the beam to be relativistic, the first term in the brackets is ignorable, accelerations that are perpendicular to the velocity being much more efficient producers of radiation than parallel accelerations. In the direction perpendicular to the beam,

© American Astronomical Society • Provided by the NASA Astrophysics Data System

1988ApJ...326..110B

the acceleration of each beam electron when that electron is within the electric field E of a plasma-electron clump is given by $dv_\perp/dt = -(e/\gamma m_e)E$. Since all of the electrons in a beam clump undergo the same acceleration, equation (A1) becomes

$$P = \frac{2}{3}\frac{N^2 e^4}{m_e^2 c^4}\gamma^4 E^2 , \tag{A2}$$

where $\beta \approx 1$ was used. To estimate the strength of the electric field E of an electron density clump in the plasma, the clump is taken to be a sphere of radius $r = \lambda/2$ containing a uniform charge density $e\delta n$. Integrating Coulomb's law $\nabla \cdot E = 4\pi n_q$, the maximum value $E = (2\pi/3)e\delta n\lambda$ is obtained. Also the number of electrons N in a clump is given by δn times the volume of a clump, yielding $N = \delta n(\pi/6)\lambda^3$. Inserting these E and N values into equation (A2) yields

$$P = \frac{2\pi^4}{3^5}\frac{e^6}{m_e^2 c^3}\gamma^4(\delta n)^4\lambda^8 \tag{A3}$$

for the power emitted from one beam clump. Clearly, to maximize the power estimate, the maximum value of the electrostatic wavelength λ is to be taken. This wavelength is the plasma skin depth $\lambda = c/\omega_{pe}$, which is also the wavelength of the beam-driven Langmuir wave. Using $\omega_{pe}^2 = 4\pi n_0 e^2/m_e$, this yields

$$P = \frac{1}{2^7 3^5}\frac{m_e^2 c^5}{e^2}\left(\frac{\gamma\delta n}{n_0}\right)^4 = 2.8 \times 10^{12}\ \text{ergs s}^{-1}\left(\frac{\gamma\delta n}{n_0}\right)^4 \tag{A4}$$

as the maximum power emitted per clump. An estimate of the maximum power from a plasma is given by the maximum power per clump times the number of clumps in that plasma. The number of clumps is given by the total volume occupied by clumps divided by the total volume of one clump. The occupied volume is fV_{plasma}, where f is the fraction of the volume filled by clumps and where V_{plasma} is the volume of the plasma. The volume of a clump is $(4\pi/3)\ (\lambda/2)^3$, so the number of clumps is $6fV_{plasma}/\pi\lambda^3$. Multiplying relation (A3) by this value yields

$$P = \frac{4\pi^3}{81}\frac{e^6}{m_e^2 c^3}\gamma^4(\delta n_p)^4\lambda^5 f V_{plasma} \tag{A5}$$

as the power emitted from the plasma. Again, to maximize this, $\lambda = c/\omega_{pe}$ is taken, yielding

$$P = \frac{\pi^{1/2}}{(8)(81)}ec^2 m_e^{1/2} n_0^{3/2}\left(\gamma\frac{\delta n}{n_0}\right)^4 f V_{plasma} = 3.6 \times 10^{-5}\ \text{ergs s}^{-1}\left(\frac{n_0}{\text{cm}^{-3}}\right)^{3/2}\left(\gamma\frac{\delta n}{n_0}\right)^4 f V_{plasma} \tag{A6}$$

as an estimated maximum power from a plasma of volume V_{plasma}, where n_0 is the number density of the plasma, δn is the number density amplitude of the beam-driven clumps, γ is the relativistic factor of the electron beam, and f is the filling factor of the clumps.

APPENDIX B

RELATIVISTIC BEAM–DRIVEN FIRE HOSE INSTABILITY LENGTH SCALES

To obtain an estimate for the minimum growth length of the fire hose instability, the case where the instability is driven by a cold relativistic electron beam in a nonrelativistically flowing plasma is explored. The dispersion relation for the growth of Alfvén waves is obtained as follows. As a source term for Maxwell's equations, the current density is obtained from the cold fluid equations of motion for the relativistic beam with drift velocity v_b and the plasma electrons and ions, both with drift velocities of $v_0 \ll c$. Charge neutrality is assumed; hence, the background ions are taken to have a number density of n_0, the beam is taken to have n_b, and the background electrons to have $n_e = n_0 - n_b$. Considering only electromagnetic waves that propagate parallel to the ambient magnetic induction B_0 in a homogeneous plasma, a harmonic analysis $e^{-kz-i\omega t}$ of Maxwell's equations for $\omega - kv_0 \ll \omega_{ce}$ yields the dispersion relation

$$k^2 - \frac{\omega^2}{c^2} - \frac{(\omega - kv_0)^2}{v_{Ai}^2[-(\omega - kv_0)^2/\omega_{ci}^2]} - \frac{\gamma(\omega - kv_b)^2}{v_{Ab}^2[1 - \gamma^2/\omega_{ce}^2(\omega - kv_b)^2]}$$

$$= \pm\left[\frac{\omega - kv_0}{c}\left\{-\frac{\omega_{pi}}{v_{Ai}[1 - (\omega - kv_0)^2/\omega_{ci}^2]} + \frac{\omega_{pe}}{v_{Ae}}\right\} + \frac{\omega_{pb}}{v_{Ab}c}\frac{\omega - kv_b}{1 - \gamma^2/\omega_{ce}^2(\omega - kv_b)^2}\right], \tag{B1}$$

where $v_A^2 = B_0^2/4\pi nm$ and $\omega_p^2 = 4\pi ne^2/m$, the n and m values taken appropriately for the various species. For $v_0 = v_b = 0$, dispersion relation (B1) yields the two circularly polarized branches of the Alfvén wave dispersion relation

$$\frac{\omega^2}{k^2} = v_A^2\frac{1 \pm (\omega/\omega_{ci})}{1 + v_A^2/c^2(1 \pm \omega/\omega_{ci})} . \tag{B2}$$

For $v_A^2 \ll c^2$, the one branch (lower sign) has $\omega/k \to 0$ as $\omega \to \omega_{ci}$: this describes the circularly polarized electromagnetic wave that has its electric field vector rotating in the direction of the ion gyromotion in the ambient induction $\boldsymbol{B}_0$. The other branch (upper sign)

© American Astronomical Society • Provided by the NASA Astrophysics Data System

1988ApJ...326..110B

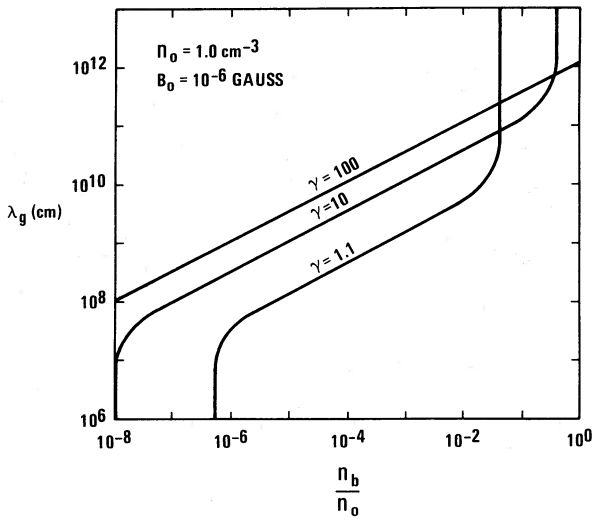

FIG. 6.—Growth scale lengths for the fire hose instability as a function of n_b/n_0, the ratio of the relativistic beam density to the background jet plasma density.

has $\omega/k \to (2)^{1/2} v_A$ for $\omega \to \omega_{ci}$ and $v_A^2 \ll c^2$: it describes the wave that has its electric field vector rotating in the electron-gyromotion direction. For $\omega \to 0$, both branches have $\omega/k \to 0$.

Dispersion relation (B1) is solved numerically for k complex and ω real, appropriate to the boundary value problem of spatially growing electromagnetic plasma waves driven by the relativistic electron beam emanating from the core source. For $v_0 \approx 0$ (very slow bulk outflow of the jet), the mode that is circularly polarized in the sense of the ion gyromotion is most easily driven unstable by the electron beam. Typically, the fastest growing wave of this branch has a frequency $\omega \approx \omega_{ci}$. The fastest growing waves of the electron-polarized branch have frequencies $\omega \gg \omega_{ci}$ (whistlers).

In Figure 6, the growth length for the ion-gyromotion polarized fire hose instability is plotted as a function of n_b/n_0 for three values of the relativistic beam γ. The frequency is taken to be $\omega = 0.95\omega_{ci}$. According to dispersion relation (B2), the instability growth is faster for $\omega \approx \omega_{ci}$ than it is at $\omega = 0.95\omega_{ci}$, but the cold fluid theory used here is invalid near $\omega \approx \omega_{ci}$ because the background ions are near cyclotron resonance with the wave and kinetic effects have been neglected. At $\omega = 0.95\omega_{ci}$, kinetic effects should be unimportant for a cold plasma; thus, the growth of the fire hose instability is at least as fast as the values plotted in Figure 6. As can be seen in the figure, for n_b/n_0 too small or too large, the beam-plasma system is fire hose stable. The lower n_b condition for instability can be written $\omega_{pb}^2 \geq \omega_{ce}^2/\gamma$, which is $\gamma n_b m_e c^2 \geq B_0^2/4\pi$. This can be interpreted as the necessity for the ram pressure of the beam to exceed the pressure of the ambient magnetic field. Note that the properties of the background plasma do not enter this turn-on condition. The upper n_b condition is more difficult to obtain. Shutdown of the fire hose instability occurs for n_b/n_0 large enough that the current density that results from the $\boldsymbol{v}_b \times \boldsymbol{B}_{wave}$ force on the relativistic beam electrons exceeds the ion polarization drift current density. If this occurs, the currents arising when the electron beam passes through the electromagnetic wave create magnetic fields that oppose and dominate the wave magnetic fields. When the beam-plasma system is fire hose unstable, the resulting electromagnetic waves have phase velocities ω/k_{real} that are much larger than the Alfvén speed of the background plasma, and the real and imaginary parts of the wavevector k are comparable in magnitude, the real part typically being $k_{real} \approx \frac{1}{2}(\omega_{ce}/\gamma v_b)$.

REFERENCES

Alfvén, H. 1978, *Ap. Space Sci.*, **54**, 279.
Alfvén, H., and Fälthammar, C.-G. 1963, *Cosmical Electrodynamics* (Oxford: London).
Allen, H. D., Aller, M. F., and Hughes, P. A. 1985, *Ap. J.*, **298**, 296.
Attwood, D., Halbach, K., and Kim, K. J. 1985, *Science*, **228**, 1265.
Baranga, A., Benford, G., and Tzach, D. 1985, *Phys. Rev. Letters*, **54**, 1377.
Bekefi, G. 1966, *Radiation Processes in Plasmas* (New York: Wiley).
Benford, G. 1978, *M.N.R.A.S.*, **183**, 29.
———. 1985, in *Physics of Energy Transport in Extragalactic Radio Sources*, ed. A. Bridle and J. Eilek (Green Bank: NRAO Press), p. 135.
Benford, G., Main, W., Baranga, A., and Kato, K. 1986, in *Proc. Beams '86 Conf.*, ed. C. Yamahaka (Kobe, Japan: Kobe University Press), p. 200.
Birn, J., Hones, E. W., Jr., Bame, S. J., and Russell, C. T. 1985, *J. Geophys. Res.*, **90**, 7449.
Blandford, R. D., and Rees, M. J. 1974, *M.N.R.A.S.*, **169**, 395.
Bridle, A. H., and Perley, R. A. 1984, *Ann. Rev. Astr. Ap.*, **22**, 319.
Browne, I. W. A., and Perley, R. A., 1986, *M.N.R.A.S.*, **222**, 149.
Carr, T. D., Desch, M. D., and Alexander, J. K. 1983, in *Physics in the Jovian Magnetosphere*, ed. A. J. Dessler (Cambridge: Cambridge University Press), p. 226.
Chen, F. F. 1984, *Introduction to Plasma Physics and Controlled Fusion*, Vol. **1** (New York: Plenum).
Dattner, A. 1962, *Ark. Fys.*, **21**, 71.
De Young, D. S. 1984, *Science*, **225**, 677.
Elder, J. W. 1960, *J. Fluid Mech.*, **9**, 235.
Elias, L. R., Fairbank, W. M., Madey, J. M. J., Schwettman, H. A., and Smith, T. I. 1976, *Phys. Rev. Letters*, **36**, 717.
Gary, S. P., Gerwin, R. A., and Forslund, D. W. 1976, *Phys. Fluids*, **19**, 579.
Goldman, M. 1984, *Rev. Mod. Phys.*, **56**, 709.
Goldstein, M. L., Smith, R. A., and Papadopoulos, K. 1979, *Ap. J.*, **234**, 683.
Gould, R. J. 1979, *Astr. Ap.*, **76**, 306.
Granatstein, V. L., and Sprangle, P. 1977, *IEEE Trans. MTT*, **25**, 545.
Heeschen, D. S. 1982, in *IAU Symposium 97, Extragalactic Radio Sources*, ed. D. S. Heeschen and C. M. Wade (Dordrecht: Reidel), p. 327.
Hewitt, R. G., Melrose, D. B., and Ronnmark, K. G. 1981, *Proc. Astr. Soc. Australia*, **4**, 221.
Hjellming, R. M., and Johnson, K. J. 1982, in *IAU Symposium 97, Extragalactic Radio Sources*, ed. D. S. Heeschen and C. M. Wade (Dordrecht: Reidel), p. 197.
Jones, M. E., Lemons, D. S., and Mostrom, M. A. 1983, *Phys. Fluids*, **26**, 2784.
Kapitza, P. L., and Dirac, P. A. M. 1933, *Proc. Cambridge Phil. Soc.*, **29**, 297.
Kato, K. G., Benford, G., and Tzach, D. 1983, *Phys. Fluids*, **26**, 3636.
Kellerman, K. I. 1985, *Comments Ap.*, **11**, 69.
Kellerman, K. I., and Pauliny-Toth, I. I. K. 1969, *Ap. J. (Letters)*, **155**, L71.
Kivelson, M. G., and Pu, Z.-Y. 1984, *Planet. Space Sci.*, **32**, 1135.
Levron, D., Benford, G., and Tzach, D., 1987, *Phys. Rev. Letters*, **58**, 1336.
Lichtenberg, W., Przybylski, A., and Scheer, M. 1975, *Phys. Rev. A*, **11**, 480.
Lovelace, R. V. E. 1976, *Nature*, **262**, 649.
Madey, J. M. J. 1971, *J. Appl. Phys.*, **42**, 1906.
Marscher, A. P. 1983, *Ap. J.*, **264**, 296.

© American Astronomical Society • Provided by the NASA Astrophysics Data System

1988ApJ...326..110B

Marscher, A. P., and Broderick, J. J. 1981, *Ap. J.*, **249**, 406.
Melrose, D. B., Hewitt, R. G., and Dulk, G. A. 1984, *J. Geophys. Res.*, **89**, 897.
Nicholson, D. R. 1983, *Introduction to Plasma Theory* (New York: Wiley).
Noerdlinger, P. D. 1968, *Phys. Rev. Letters*, **20**, 146.
Noerdlinger, P. D., and Yui, A. K.-M. 1969, *Ap. J.*, **157**, 1147.
Owen, F. N. 1986, in *IAU Symposium 119, Quasars*, ed. G. Swarup and V. K. Kapahi (Dordrecht: Reidel), p. 173.
Pantell, R. H., Soncini, G., and Puthoff, H. E. 1968, *Proc. IEEE J. Quant. Electron.*, **4**, 905.
Peacock, J. A., Miller, L., and Longair, M. S. 1986, *M.N.R.A.S.*, **218**, 265.
Polymeropoulos, C. E., and Gebhart, B. 1967, *J. Fluid Mech.*, **30**, 225.
Simonetti, J. H., Cordes, J. M., and Heeschen, D. S. 1985, *Ap. J.*, **296**, 46.
Spangler, S. R. 1979, *Ap. J. (Letters)*, **232**, L7.
Sprangle, P., and Drobot, A. T. 1977, *Proc. IEEE Trans. Microwave Theory Tech.*, **MTT-25**, 528.
Urry, C. M., and Mushotzky, R. F. 1982, *Ap. J.*, **253**, 38.
Windsor, R. A., and Kellogg, P. J. 1974, *Ap. J.*, **190**, 167.
Wu, C. S., and Lee, L. C. 1979, *Ap. J.*, **230**, 621.
Zakharov, V. E. 1972, *Soviet Phys.—JETP*, **35**, 908.

DANIEL N. BAKER: Code 690, NASA/Goddard Space Flight Center, Greenbelt, MD 20771

GREGORY BENFORD: Department of Physics, University of California, Irvine, CA 92717

JOSEPH E. BOROVSKY: Space Plasma Physics Group, Mail Stop D438, Los Alamos National Laboratory, Los Alamos, NM 87545

JEAN A. EILEK: Physics Department, New Mexico Institute of Mining and Technology, Socorro, NM 87801

© American Astronomical Society • Provided by the NASA Astrophysics Data System